

Ago2 facilitates Rad51 recruitment and DNA double-strand break repair by homologous recombination

Min Gao^{1,4,*}, Wei Wei^{2,3,*}, Ming-Ming Li^{1,4,*}, Yong-Sheng Wu^{1,*}, Zhaoqing Ba^{2,3}, Kang-Xuan Jin^{1,4}, Miao-Miao Li^{1,4}, You-Qi Liao^{1,4}, Samir Adhikari^{1,4}, Zechen Chong¹, Ting Zhang¹, Cai-Xia Guo¹, Tie-shan Tang⁵, Bing-Tao Zhu⁶, Xing-Zhi Xu⁶, Niels Mailand⁷, Yun-Gui Yang^{1,4}, Yijun Qi^{2,3}, Jannie M Rendtew Danielsen^{1,7}

¹Laboratory of Genome Variations and Precision Biomedicine, Beijing Institute of Genomics, Chinese Academy of Sciences, Beijing 100101, China; ²Tsinghua-Peking Center for Life Sciences, Beijing 100084, China; ³Center for Plant Biology, School of Life Sciences, Tsinghua University, Beijing 100084, China; ⁴University of Chinese Academy of Sciences, Beijing 100049, China; ⁵State Key Laboratory of Biomembrane and Membrane Biotechnology, Institute of Zoology, Chinese Academy of Sciences, Beijing 100101, China; ⁶Beijing Key Laboratory of DNA Damage Response, College of Life Sciences, Capital Normal University, Beijing 100048, China; ⁷The Novo Nordisk Foundation Center for Protein Research, Ubiquitin Signalling Group, Faculty of Health Sciences, Copenhagen, Denmark

DNA double-strand breaks (DSBs) are highly cytotoxic lesions and pose a major threat to genome stability if not properly repaired. We and others have previously shown that a class of DSB-induced small RNAs (diRNAs) is produced from sequences around DSB sites. DiRNAs are associated with Argonaute (Ago) proteins and play an important role in DSB repair, though the mechanism through which they act remains unclear. Here, we report that the role of diRNAs in DSB repair is restricted to repair by homologous recombination (HR) and that it specifically relies on the effector protein Ago2 in mammalian cells. Interestingly, we show that Ago2 forms a complex with Rad51 and that the interaction is enhanced in cells treated with ionizing radiation. We demonstrate that Rad51 accumulation at DSB sites and HR repair depend on catalytic activity and small RNA-binding capability of Ago2. In contrast, DSB resection as well as RPA and Mre11 loading is unaffected by Ago2 or Dicer depletion, suggesting that Ago2 very likely functions directly in mediating Rad51 accumulation at DSBs. Taken together, our findings suggest that guided by diRNAs, Ago2 can promote Rad51 recruitment and/or retention at DSBs to facilitate repair by HR.

Keywords: Rad51; Ago2; diRNA; Homologous recombination; DSB

Cell Research (2014) 24:532-541. doi:10.1038/cr.2014.36; published online 25 March 2014

Introduction

DNA double-strand breaks (DSBs) are highly cytotoxic lesions and pose a major threat to genome stability if not properly repaired [1-4]. DSBs are primarily repaired by non-homologous end joining (NHEJ) or homologous recombination (HR). Whereas NHEJ is efficient but error prone in piecing the DNA ends together, HR allows faithful repair, but requires sister chromatids and is there-

fore restricted to S and G2 [5-7]. HR repair is initiated by resection of DSB ends by the Mre11-Rad50-Nbs1 (MRN) complex, CtBP-interacting protein (CtIP) and Exonuclease 1 (EXO1) to generate single-stranded DNA (ssDNA) that gets coated with the trimeric single strand-binding protein complex Replication protein A (RPA) [8-11]. RPA is then replaced by Rad51 to form nucleoprotein filaments that facilitate strand invasion and initiate the HR process [6].

Small RNAs (sRNAs) have emerged as important players in various aspects of biology. They are processed from double-strand RNAs by Dicer and associate with the Argonaute (Ago) family of proteins [12]. We have previously demonstrated that a class of sRNAs can be produced from the sequences in the vicinity of DSB sites in *Arabidopsis thaliana* and humans [4]. These DSB-

*These four authors contributed equally to this work.

Correspondence: Yijun Qi^a, Yun-Gui Yang^b

^aE-mail: qiyijun@tsinghua.edu.cn

^bE-mail: ygyang@big.ac.cn

Received 8 November 2013; revised 10 January 2014; accepted 27 January 2014; published online 25 March 2014

induced sRNAs or diRNAs are associated with Ago proteins and required for DSB repair [4]. Similar site-specific Dicer- and Drosha-dependent sRNAs (named DDRNAs) have been found in vertebrates and suggested to be involved in DNA damage response (DDR) signaling and activation [13]. DSB-derived sRNAs have also been detected in fly cells [14]. How diRNAs facilitate repair remains largely unknown. In this study, we sought to examine whether diRNAs facilitate DSB repair through facilitating the recruitment of repair proteins to DSB sites. We found that Ago2 interacts with Rad51 and is required for Rad51 accumulation at DSB sites. Interestingly, small RNA binding and catalytic activity of Ago2 are dispensable for the Ago2-Rad51 interaction but indispensable for Rad51 recruitment and HR repair. These findings support a model in which Rad51 is guided to DSB sites by diRNAs through interacting with Ago2.

Results

The role of diRNAs in DSB repair is restricted to repair by HR and specifically relies on Ago2

We have previously shown that diRNAs function through Ago proteins and depletion of Ago2 in human cells results in a significant reduction in repair by HR [4]. Here we first examined whether in humans, other Ago-clade members could also be involved in HR repair using the DR-GFP/U2OS HR reporter system. In this system, U2OS cells carry a DR-GFP substrate, which contains two nonfunctional GFP open-reading frames, including one GFP-coding sequence that is interrupted by a recognition site for the *I-SceI* endonuclease. Expression of *I-SceI* leads to formation of a DSB in the *I-SceI* GFP allele, which can be repaired by HR using the nearby GFP sequence lacking the N- and C-termini, thereby producing functional GFP that can be readily detected by flow cytometry [15]. Consistent with our previous findings [4], depletion of Ago2, Dicer or Drosha/DGCR8 impaired HR to a similar degree as Rad51 knockdown (Figure 1A, Supplementary information, Figure S1A and S1B). However, depletion of any of the other Ago homologs (Ago1, Ago3 and Ago4) had no detectable effect on HR efficiency (Figure 1A, Supplementary information, Figure S1A, S1C and S1D), showing that the function of diRNAs in HR repair specifically relies on Ago2. The decrease in HR repair could not be explained by differences in cell cycle distribution (Supplementary information, Figure S1E). Furthermore, we tested the expression of several key DNA damage response and repair factors and their expression remained unaltered by depletion of Ago2 or Dicer, except for a minor decrease in Chk2 following prolonged depletion (Supplementary information,

Figure S1F). Strikingly, we found that HR repair could be restored in Dicer-depleted cells by incubation with sRNAs isolated from *I-SceI*-transfected U2OS/DR-GFP cells (Figure 1B and Supplementary information, Figure S1G), demonstrating a direct role for diRNAs in HR repair. Surprisingly, sRNAs isolated from control cells containing no *I-SceI* had a weak rescuing effect on HR, suggesting that in addition to diRNAs some DNA damage-independent sRNA species might also be involved.

Next, we tested the impact of diRNAs on NHEJ using a well-established NHEJ reporter assay [16]. Interestingly, in contrast to HR, NHEJ was not affected by depletion of either Ago2 or Dicer (Figure 1C and Supplementary information, Figure S1H), demonstrating that the function of diRNAs in DSB repair is restricted to the repair by HR. Since the NHEJ assay does not distinguish between repairs by classical or alternative NHEJ, we cannot rule out the possibility that the ratio between these two repair pathways might be affected.

A previous report suggests that Drosha and Dicer are required for DNA damage response signaling [13]. However, in our experimental settings, we did not observe defects in the recruitment of DNA damage signaling proteins in general or in checkpoint activation following Ago2 or Dicer depletion (Supplementary information, Figures S2, S3 and S4A, S4C-S4F). Taken together, these data solidify the conclusion that in association with Ago2, diRNAs play a specific role in HR repair.

Ago2 interacts with Rad51

How do Ago2 and diRNAs facilitate HR repair? Several reports suggest that non-coding RNAs can target proteins to specific genomic loci to induce histone modifications and affect transcription patterns [17-20]. We have previously proposed that Ago2/diRNAs may recruit chromatin-modifying complexes to modify local chromatin or directly recruit proteins required for HR repair at DSB sites to facilitate repair [4]. To test the latter possibility, we sought to examine whether Ago2 accumulates at DSB sites and interacts with any of the proteins involved in the DNA damage response using chromatin immunoprecipitation (ChIP) analysis and co-immunoprecipitation experiments. By using the DR-GFP/U2OS HR reporter system [15], we could show enrichment of Ago2 at DSBs (Figure 2A and 2B), suggesting that Ago2 is recruited to sites of DNA damage. Most intriguingly, overexpressed as well as endogenous Ago2 interacted with Rad51, but not with other tested DNA damage-related proteins including Mdc1, 53BP1 and RPA (Figure 2C). The association between Ago2 and Rad51 was enhanced by treatment with ionizing radiation (IR) which generates DSBs (Figure 2F), suggesting importance of the Ago2-

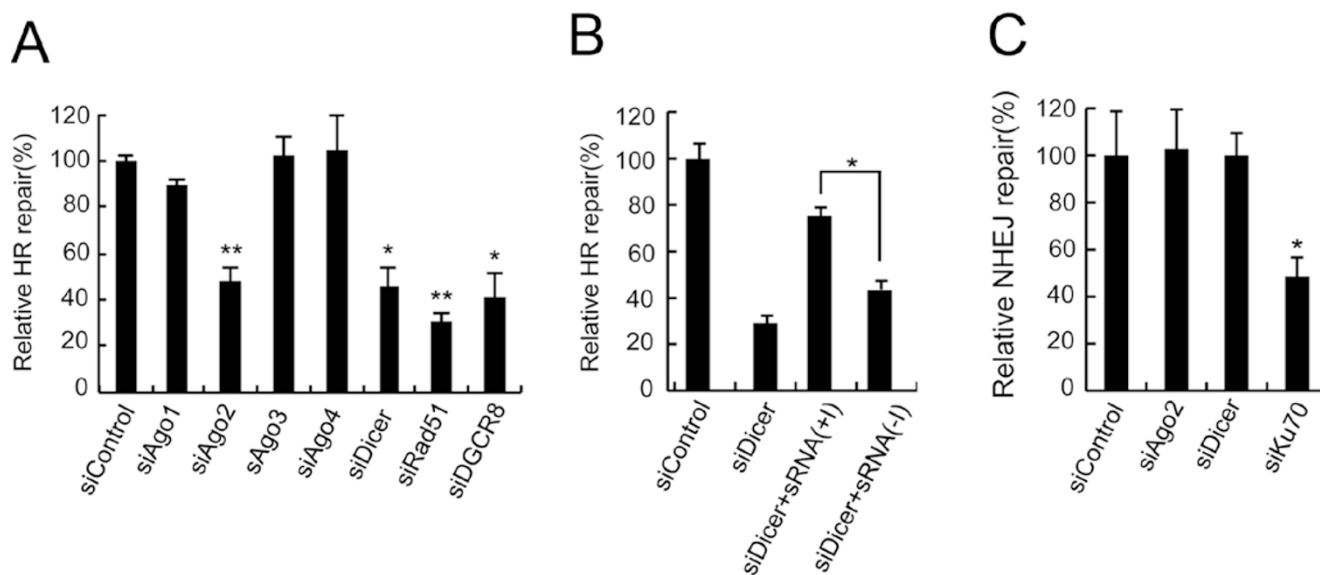


Figure 1 The role of diRNAs in DSB repair is restricted to repair by HR and specifically relies on Ago2. **(A)** HR repair rates in U2OS/DR-GFP cells treated with the indicated siRNAs. **(B)** HR repair was restored by incubation with 50 ng of sRNAs (0.25 ng/ μ l) prepared from U2OS/DR-GFP cells transfected with pCBA-I-SceI (+) but not empty vector (-) in Dicer-knockdown cells. **(C)** NHEJ repair rates in HEK 293/EJ5-GFP cells treated with the indicated siRNAs. Knockdown of Ku70 that is important for NHEJ, but not Dicer or Ago2, reduced NHEJ. (* $P < 0.005$, ** $P < 0.0001$, Student's t -test). The number of GFP-positive cells was measured by flow cytometry and the repair efficiency was scored as the percentage of GFP-positive cells. The extent of repair is shown relative to the repair observed in cells treated with control siRNAs. Histograms represent the mean of three independent experiments. Data are represented as mean \pm SEM.

Rad51 interaction in DSB repair.

Ago2 and Dicer are required for Rad51 recruitment to DSBs

The finding that Ago2 interacts with Rad51 prompted us to test whether the recruitment of Rad51 to DSBs depends on Ago2/diRNAs. To this end, we examined the localization of Rad51 at DSB sites in Ago2- or Dicer-depleted cells. Following the knockdown of Ago2 or Dicer by specific siRNAs, Rad51 but not γ H2AX (the phosphorylated form of H2AX that enriches at DSBs) focus formation was severely impaired in IR-treated cells (Figure 3A, 3B and Supplementary information, Figure S4B) [21, 22]. The overall Rad51 protein level was unaltered by Ago2 or Dicer knockdown (Figure 3C). Likewise, in *Ago2*^{-/-} MEF cells [23] the recruitment of Rad51 to DSB tracks generated by micro-laser irradiation was strongly reduced (Figure 3D). Since Rad51 recruitment relies on the previous resection of DSBs that generates 3' overhangs, the defect in Rad51 focus formation might be explained by impaired resection in Ago2- or Dicer-depleted cells. However, DNA end-resection appeared normal as judged by the amount of ssDNA detected in Ago2 or Dicer knockdown cells following CPT treatment (Figure

4A and 4B). In addition, Mre11 and RPA accumulated normally at DSB sites in Ago2 or Dicer knockdown cells (Figure 4C-4F). Taken together, these results suggest that Ago2/diRNAs facilitate Rad51 recruitment to DSBs, very likely through the interaction of Rad51 with Ago2.

DiRNA binding and catalytic activity of Ago2 are dispensable for the interaction with Rad51

We next investigated whether the Ago2-Rad51 interaction requires diRNAs. We found that preventing diRNA generation by depletion of Dicer did not reduce the interaction between Ago2 and Rad51, suggesting that diRNAs are not necessary for efficient Ago2-Rad51 interaction (Figure 5A). To confirm this, we used an sRNA-binding deficient Ago2 mutant (Y311A/F312A or YA/FA), in which two conserved residues important for sRNA-binding were substituted with alanine [24]. Consistent with our observation in Dicer-depleted cells, wild-type and YA/FA mutant Ago2 associated equally well with Rad51 (Figure 5B), indicating that sRNA binding is not necessary for Ago2 to interact with Rad51. Ago2 possesses a functional catalytic core containing three key residues (D597, D669 and H807) [25]. We found that a point mutation in the catalytic triad (D669A) had no

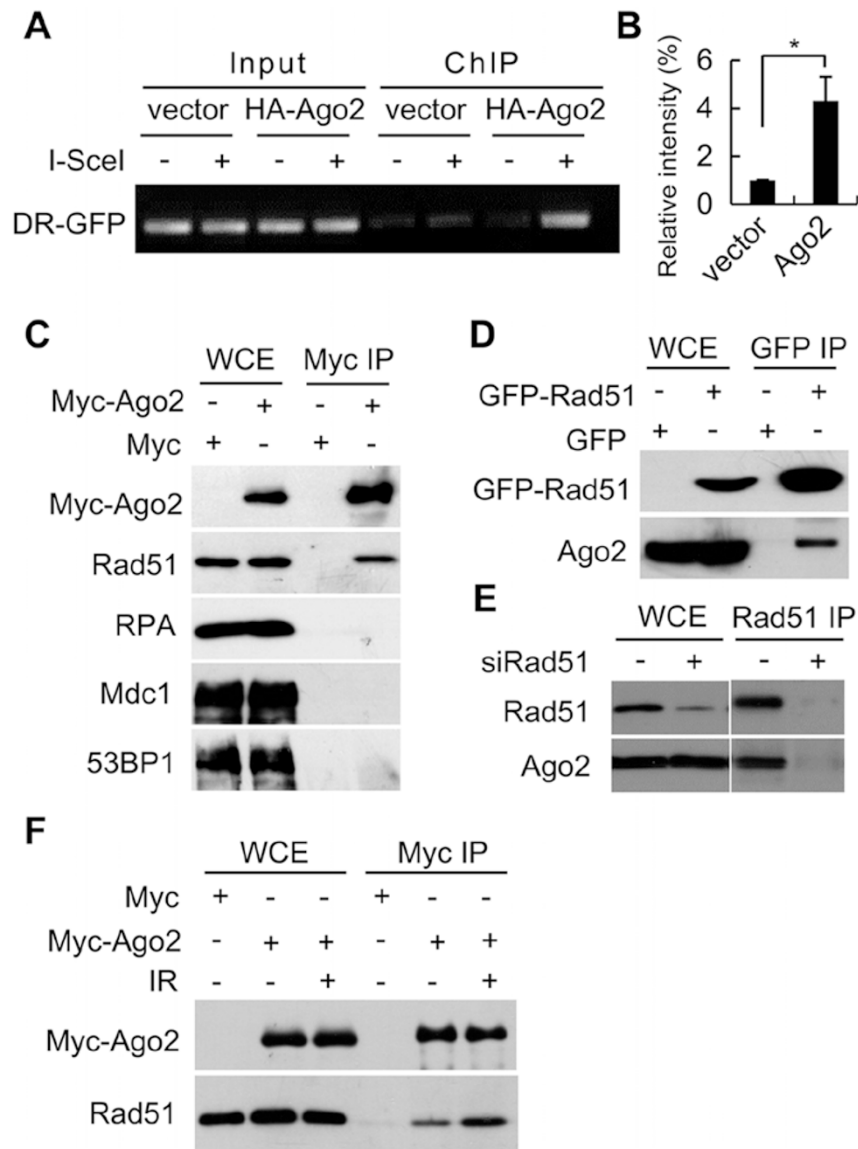


Figure 2 Ago2 accumulates at DSBs and interacts with Rad51. **(A)** U2OS/DR-GFP cells were transfected with empty vector or HA-Ago2 constructs, followed by transfection with I-SceI or empty vector control. ChIP assays were performed using HA antibody. Bound DNA was analyzed by PCR. **(B)** Quantification of ChIP data shown in **A**. The quantification is based on three independent experiments. Data are represented as mean \pm SEM. **(C)** Myc-Ago2 or empty vector were overexpressed in 293T cells by transfection as indicated and the lysates were subjected to immunoprecipitation using Myc-coupled beads. Immunoprecipitates (IP) and whole-cell extracts (WCE) were immunoblotted with the indicated antibodies. **(D)** GFP-Rad51 was overexpressed in 293T cells by transfection as indicated and the lysates were subjected to immunoprecipitation using GFP beads. Immunoprecipitates and WCE were immunoblotted with the indicated antibodies. **(E)** 293T cells were transfected with control or Rad51 siRNAs, lysed and the lysates were subjected to Rad51 immunoprecipitation. Immunoprecipitates and WCE were immunoblotted with the indicated antibodies. **(F)** Two days post transfection with the indicated DNA constructs, 293T cells were treated with IR (5 Gy) and left to recover for 1 h. Cells were then lysed and the lysates were subjected to immunoprecipitation using Myc-beads. Immunoprecipitates and WCE were immunoblotted with the indicated antibodies (* $P < 0.005$, Student's *t*-test).

obvious effect on Ago2 binding to Rad51 (Figure 5B), suggesting that catalytic activity like sRNA binding is dispensable for the interaction between Ago2 and Rad51.

DiRNA binding and catalytic activity of Ago2 are required for recruitment of Rad51 to DSBs

Though not essential for the Ago2-Rad51 interaction,

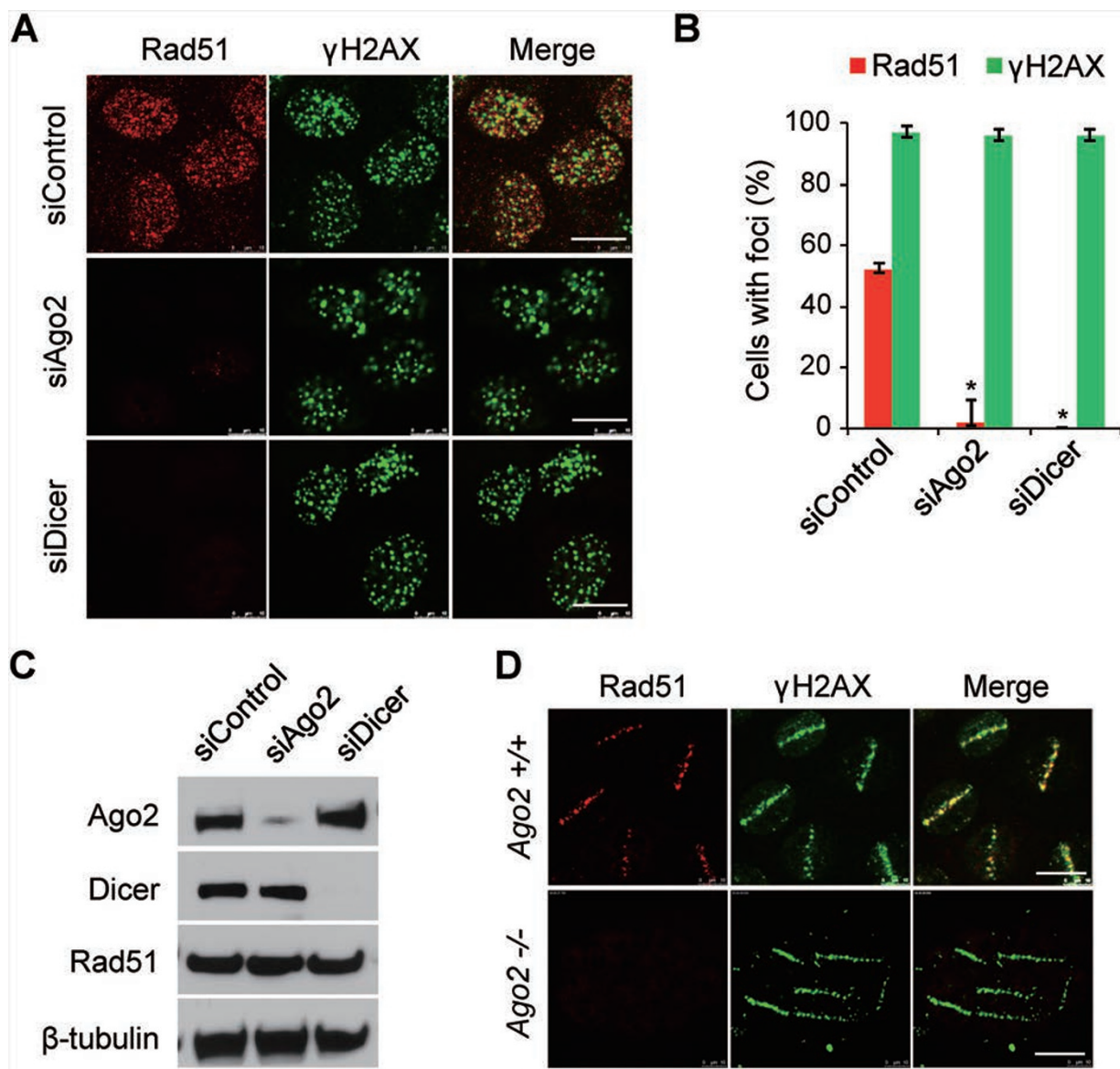


Figure 3 Ago2 and Dicer are required for Rad51 recruitment to DSBs. **(A)** U2OS cells were transfected with the indicated siRNAs for 48 h. Then, cells were treated with IR (5 Gy) and 1 h later immunostained with the indicated antibodies. Scale bars, 20 μ m. **(B)** Quantification of cells positive for Rad51 and γ H2AX. Data from three independent experiments were used to generate the histogram. Data are represented as mean \pm SEM. **(C)** U2OS cells were treated with the indicated siRNAs for 48 h, lysed and the lysates were subjected to immunoblotting with the indicated antibodies. **(D)** Wild-type or *Ago2*^{-/-} MEF cells grown on microlaser dishes were treated with 10 μ M BrdU for 24 h. The cells were then subjected to microirradiation with pulsed UVA laser ($\lambda = 365$ nm), and 1 h later immunostained with Rad51 and γ H2AX antibodies. Scale bars, 20 μ m. See also Supplementary information, Figure S5A and S5B. **P* < 0.005, Student's *t*-test.

we next tested if diRNA binding and catalytic activity of Ago2 are required for the recruitment of Rad51 to DSBs. As already shown, knockdown of Dicer, and hence prevention of diRNA generation, abrogates Rad51 focus formation following DNA damage (Figure 3A and 3B). Importantly, complementation of Ago2-knockdown cells with wild-type Ago2, but not YA/FA or D669A mutants,

restored Rad51 focus formation (Figure 5C, Supplementary information, Figure S5A and S5B). Similarly, we found, by using the HR reporter system, that complementation of Ago2-knockdown cells with wild-type Ago2, but not YA/FA or D669A mutants, rescued HR repair (Figure 5D and Supplementary information, Figure S5B), indicating that Ago2 needs its ability to associate

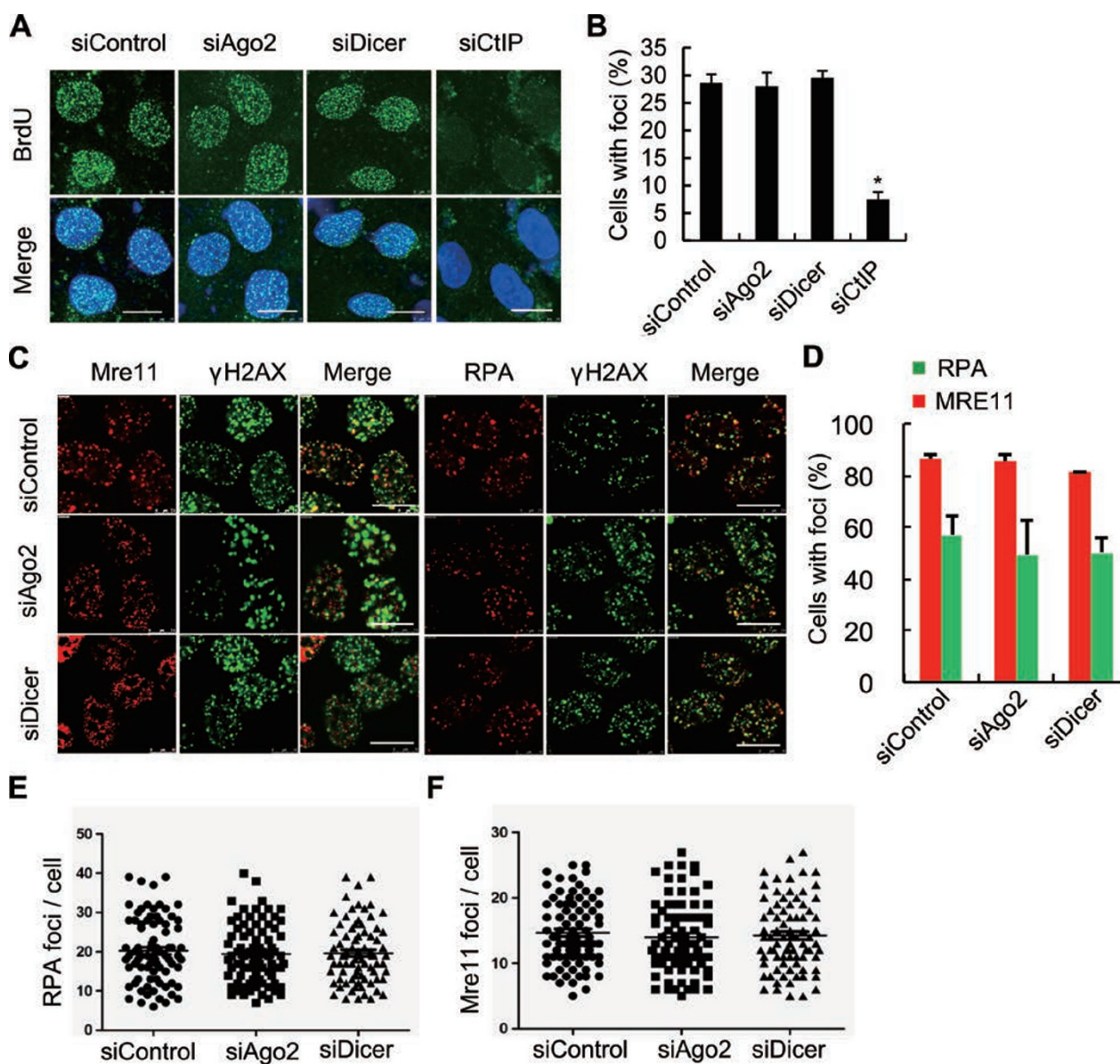


Figure 4 Ago2 and Dicer are not involved in DNA end resection or RPA/Mre11 foci formation. **(A)** U2OS cells were treated with the indicated siRNAs for 48 h and labeled with 10 μ M BrdU for 36 h. CPT (5 μ M) was then added and the cells were incubated for another 2 h. Cells were immunostained with BrdU antibody and mounted in DAPI-containing mounting medium. Scale bar, 20 μ M. **(B)** Quantification of BrdU foci shown in **A**. The histogram is based on data from three independent experiments. Data are represented as mean \pm SEM. **(C)** U2OS cells were transfected with the indicated siRNAs for 48 h and then treated with IR (5 Gy). After 1 h, cells were immunostained with the indicated antibodies. Scale bars 20 μ M. **(D)** Quantification of cells with RPA and Mre11 foci shown in **C**. The histogram is based on data from three independent experiments. Data are represented as mean \pm SEM. **(E-F)** Quantification of the number of RPA and Mre11 foci per cell. At least 80 cells were quantified for each condition ($*P < 0.005$, Student's *t*-test).

with sRNA as well as its catalytic activity in order to support Rad51 recruitment to sites of DNA damage and DSB repair.

Discussion

Rad51 is recruited onto RPA-coated ssDNAs through a process facilitated by various mediator proteins [6, 7]. In this study, we demonstrate that Rad51 interacts with Ago2 (Figure 2) and Ago2 is required for the recruitment of Rad51 to DSBs (Figure 3). This provides a novel

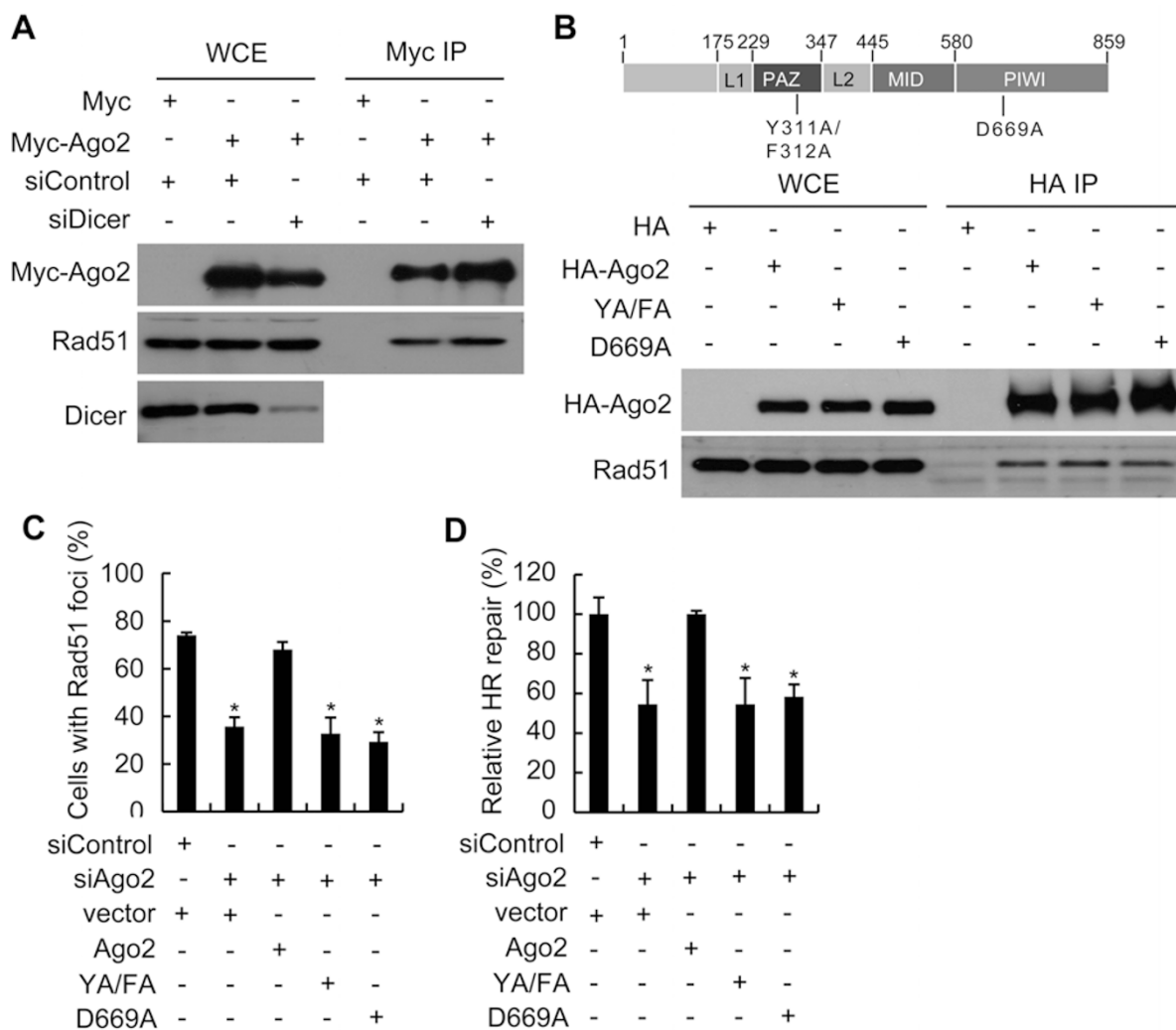


Figure 5 DiRNA binding and catalytic activity of Ago2 are required for Rad51 recruitment and HR, but are dispensable for Ago2-Rad51 interaction. **(A)** 293T cells were transfected with the indicated siRNAs and DNA constructs for 48 h, lysed and the lysates were subjected to immunoprecipitation using Myc-coupled beads. Immunoprecipitates and WCE were analyzed by immunoblotting with the indicated antibodies. **(B)** Upper panel, diagram showing the Ago2 domain structure. Y311A/F312A and D669A indicate the mutations generated to produce RNA-binding deficient and catalytically inactive mutants, respectively. Lower panel, 293T cells were transfected with the indicated constructs and lysates were subjected to immunoprecipitation with HA-coupled beads. Immunoprecipitates and WCE were immunoblotted with the indicated antibodies. **(C)** Rad51 focus formation was restored in Ago2-knockdown cells by expression of siRNA-resistant wild-type Ago2 but not Y311A/F312A or D669A mutants. The histogram is based on data from three independent experiments. Data are represented as mean \pm SEM. For representative pictures of immunostained cells, see Supplementary information, Figure S5A. **(D)** HR repair was restored in Ago2-knockdown cells by expression of siRNA-resistant wild-type Ago2 but not Y311A/F312A or D669A mutants. The extent of repair is shown relative to the repair observed in cells treated with control siRNAs. Data from three independent experiments were used to generate the histogram. Data are represented as mean \pm SEM (* $P < 0.005$, Student's *t*-test).

link between DNA repair and the RNAi machinery. Intriguingly, diRNAs are not necessary for the Ago2-Rad51 interaction (Figure 5A and 5B), but are required for Rad51 focus formation (Figure 5C) and efficient HR (Figure 5D). siRNAs are loaded onto Ago2 as duplexes, then Ago2 uses its catalytic activity to cleave the pas-

senger strand to form a mature complex containing only the guide strand [25]. Interestingly, Ago2 catalytic activity is indispensable for Rad51 focus formation (Figure 5C and Supplementary information, Figure S3A) and HR (Figure 5D), demonstrating that diRNAs most likely needs to be in a single-strand configuration to support

Rad51 accumulation and subsequent repair. Considering these observations and the fact that diRNAs are generated from sequences flanking DSBs [4, 13], Ago2-Rad51 complexes might be guided to DSB sites through base pairing between diRNAs and homologous DNA sequences surrounding the break site or scaffold RNA transcripts generated from around the break site. Base pairing between diRNAs and DNA sequences or RNA transcripts could also provide means of stabilization/retention of the DNA repair intermediate (Figure 6). Alternatively, Ago2/diRNA complexes may act to degrade nascent aberrant RNAs synthesized from broken DNA templates, thus preventing interference by these aberrant RNAs with the repair process.

Of the four Ago-clade proteins in mammals, only Ago2 has catalytic activity [23, 26]. Each of the four Ago proteins can bind miRNAs and regulate miRNA targets through mRNA deadenylation and translation inhibition, which do not require the catalytic activity of Ago2 [27]. Our finding that the catalytic activity of Ago2 is indispensable for its function in Rad51 recruitment and HR repair may help explain how an evolutionary pressure to maintain a catalytically active Ago protein in mammals is generated.

Materials and Methods

Cell culture

Human U2OS cells, 293T cells, U2OS/DR-GFP cells [28], *Ago2*^{-/-} MEF cells [23] were grown in Dulbecco's modified Eagle's medium (DMEM) at 37 °C, 5% CO₂ with 10% fetal bovine serum and 1% penicillin/streptomycin (Invitrogen). The HEK 293/EJ5-GFP cells [16] were cultured in high-glucose DMEM without phenol red containing 10% fetal bovine serum and 1% penicillin/streptomycin (Invitrogen). HEK293/EJ5-GFP cells were cultured on plates treated with 0.01% polylysine (Sigma). The following drugs were used to treat cells: Camptothecin (CPT, Sigma, 2 μM) and BrdU (Sigma, 10 μM) at the indicated times.

DNA constructs

The following DNA constructs were used in this study: Myc-Ago2, HA-Ago2, HA-Ago2Y311A/F312A, HA-Ago2D669A and GFP-Rad51. The Myc-Ago2 construct was previously described [23]. To create pcDNA3-HA-Ago2, pcDNA3-HA-Ago2Y311A-F312A and pcDNA3-HA-Ago2D669A, full-length human Ago2 was amplified and then cloned into pMD19-T (TaKaRa) with *Eco*RI and *Not*I. Y311A/F312A and D669A mutants were generated by site-directed mutagenesis using pMD19-T-Ago2 as template and confirmed by DNA sequencing. All the Ago2 forms were then introduced into pcDNA3-HA vector with *Eco*RI and *Not*I. GFP-Rad51 was constructed by cloning Rad51 cDNA into the *Bg*III and *Bam*HI sites of pEGFP-C1 (Clontech).

The following oligos were used for cloning and site-directed mutagenesis: Ago2-*Eco*RI-F: 5'-gactGAATTCgATGTACTC-GGGAGCCGCCCCGACT-3', Ago2-*Not*I-R: 5'-gactGCG-

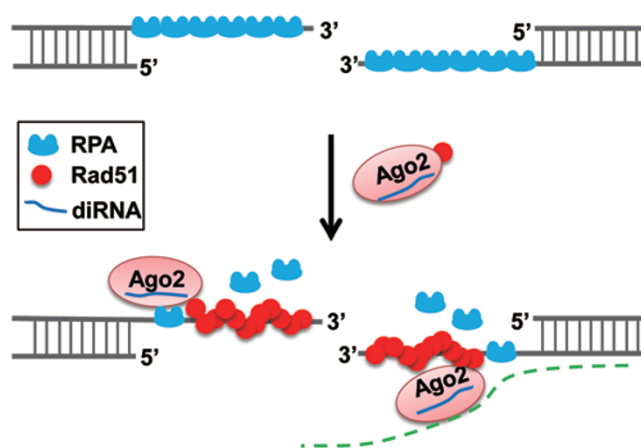


Figure 6 Working model for diRNA-directed Rad51 recruitment. Ago2-Rad51 complexes may be recruited to DNA DSB site through base pairing between diRNAs and homologous DNA sequences surrounding the break site or scaffold RNA transcripts (green dashed line) generated from DNA around the break site.

GCCGCTCAAGCAAAGTACATGGTG-3', Y311AF312A-S: 5'-TGGAGTGCACGGTGGCCCAGGCTGCCAAGGACAG-GCACAAGTTGG-3', Y311AF312A-AS: 5'-CCAACTTGT-GCCTGTCTTGGCAGCCTGGGCCACCGTGCACTCCA-3', D669A-S: 5'-CGCATCATCTTCTACCGCGCCGTGTCTCT-GAAGGCCAG-3', D669A-AS: 5'-CTGGCCTTCAGAGACAC-CGGCGCGTAGAAGATGATGCG-3', Rad51-*Bg*III-F: 5'-gactAGATCTATGGCAATGCAGATGCAGCTTG-3', and Rad51-*Bam*HI-R: 5'-gactGGATCCGTCTTGGCATCTCCCACTCC-3'.

RNAi

The following siRNAs were used to knockdown the indicated genes: Ago1 (5'-UUCUUGAGCACCUUCUCUCdTdT-3', 5'-CCAUUGUAGAACUGUUUCCdTdT-3', 5'-UAUCCAGUGAGGUAACAGCdTdT-3' and 5'-AUGCUAUGAAAGUAACUCCdTdT-3') [26], Ago2 (5'-UGACAUUGGGUUCUCAUCdTdT-3') [26], Ago3 (5'-UUACCAAUCUGCUAAUUUCdTdT-3', 5'-UUGUGCUAAAGGUAUCUUGdTdT-3', 5'-UCAUAUUGCAUAAUGAUGCdTdT-3' and 5'-UUUGCAAAGAUAGUUGUGCdTdT-3') [26], Ago4 (5'-AUUGCUAUUAGUUCUGGCCdTdT-3' and 5'-UAAUAGAUGAUCCGAGUGGdTdT-3', 5'-UCAUACUGAAAUCUCAUCdTdT-3' and 5'-UAAGGAAGCAUCCUGGUUCdTdT-3') [26], Rad51 (5'-GGCAGUAGAUGUGCAGAUAdTdT-3', 5'-GGGACAU-GCUGCUACAAUAdTdT-3', 5'-CUGCUACAAUACGGCUAAUdTdT-3'), Dicer (5'-UCCAGAGCUGCUUCAAGCAdTdT-3') [29], Ku70 (5'-UGAGUGAGUAGUCAGAUC-GUdTdT-3') [30], CtIP (5'-UAGUUUUGUCCAAAGGU-CCdTdT-3' and 5'-GAUUCGUUCCUUUUAGCdTdT-3') [31], DGCR8 (5'-AUCCGUUGAUCUCGAGGAAdTdT-3', 5'-AACAUUCGGACAAGAGUGUGAUdTdT-3', 5'-AUCACACUCUUGUCCGAUGdTdT-3') and control(5'-UAGAACGUCUAGGUAUCCdTdT-3').

All siRNA duplexes purchased from GenePharma were transfected into cells using Lipofectamine RNAiMAX (Invitrogen) according to the manufacturer's instructions.

RNA preparation

U2OS cells were treated with or without IR (5 Gy) and cultured for an additional 1 h before RNA extraction. U2OS/DR-GFP cells were transfected with I-SceI plasmid for 1 day before RNA was extracted. Total RNA was extracted with Trizol reagent (Invitrogen) according to the manufacturer's instructions. To isolate the 18-28 nt sRNA fraction, total RNA samples were separated on 15% denaturing polyacrylamide gel and the gel slices corresponding to the size of 18-28 nt sRNAs were excised. RNA was eluted from the gel with 0.4 M NaCl overnight at room temperature with agitation. After centrifugation, the supernatant was collected and RNA was precipitated and dissolved in RNase-free water.

HR and NHEJ repair reporter assays

The U2OS/DR-GFP [28] and HEK293/EJ5-GFP [16] cell lines were used for assaying HR and NHEJ repair efficiencies, respectively. Cells were transfected with a plasmid expressing I-SceI (pCBASce) for 48 h. Cells transfected with an empty vector were used as a negative control. GFP-positive cells were identified and quantified by flow cytometry. The repair efficiency was scored as the percentage of GFP-positive cells. To examine the role of individual genes in DSB repair, prior to the transfection with pCBASce, cells were treated with siRNAs specifically targeting each gene for 48 h.

Immunoprecipitation

Whole-cell extract (WCE) was generated by lysing cells in NET 0.1% buffer (50 mM Tris-HCl pH 7.4, 150 mM NaCl, 5 mM EDTA, 0.1% NP-40 and protease inhibitors) followed by sonication using a SonicDismembrator (Fisher Scientific) (1 min, with 10s-on and 20s-off cycles). Anti-HA affinity gel (Sigma, E6779), anti-Myc affinity gel (Sigma, E6654) and GFP-Trap-A beads (ChromoTek, gta-20) were used for immunoprecipitation of HA-, Myc- and GFP-tagged proteins, respectively. The beads were incubated with WCE for 5 h on a spinning wheel at 4 °C. For endogenous protein pull-down, specific antibodies were added to the WCE and incubated at 4 °C for 3 h. Then, protein A beads (Sigma, P9424) or protein G beads (Sigma, P3296) were added and the samples were incubated for additional 2 h. After incubation, the beads were washed for three times and boiled in SDS loading buffer. The samples were then separated on SDS-PAGE and subsequently subjected to immunoblotting.

Immunoblotting

Whole-cell extract prepared in RIPA buffer (20 mM Tris-HCl, pH 7.4, 20% glycerol, 0.5% NP-40, 1 mM MgCl₂, 0.5 M NaCl, 1 mM EDTA, 1 mM EGTA and protease inhibitors) or immunoprecipitates were separated on SDS-PAGE, transferred to PVDF membrane, incubated with the indicated antibodies and detected by ECL Western Blotting Detection Kit (BD Bioscience). The following antibodies were used for western blotting and immunoprecipitation: rabbit anti-Ago2/eIF2C2 antibody (Abcam, ab32381), mouse Ago1 antibody (Milipore, 04-083), mouse Ago 3 antibody (Novus, L021V1), mouse Ago4 antibody (Milipore, 05-967), mouse anti-Dicer antibody (Abcam, ab14601), rabbit anti-

Rad51(H-92) antibody (SantaCruz, sc-8349), anti-ATM antibody (Abcam, ab81292), rabbit anti-Mre11 antibody (Novus, NB100-142), mouse anti-RPA antibody (Abcam, ab2175), mouse anti-Ku70 antibody (SantaCruz, sc-5309), mouse anti-β-tubulin antibody (Sigma, T5293), rabbit anti-Myc antibody (Abcam, ab9106), mouse anti-MDC1 antibody (Abcam, ab50003), rabbit anti-53BP1 antibody (Bethyl, A300-272A), mouse anti-GFP antibody (CW-BIO, CW0258), anti-mouse IgG-HRP antibody (Dakocytomation, p0161) and anti-rabbit IgG-HRP antibody (Dakocytomation, p0448).

Immunofluorescence

U2OS cells were grown on coverslips or microlaser dishes, fixed with 4% paraformaldehyde for 15 min at room temperature and permeabilized in 0.2% Triton X-100 for 10 min at room temperature. Treated cells were then incubated with primary antibodies for 1 h at 37 °C, washed and incubated with secondary antibody for 1 h at 37 °C. The slides were mounted in Vectashield mounting medium with DAPI (Vector Laboratories). Confocal images were acquired on Leica TCS SP5 (Leica). Image analysis was carried out with SP5 image software. The following antibodies were used for immunofluorescence: rabbit anti-Rad51 (H-92) antibody (SantaCruz, sc-8349), rabbit anti-Mre11 antibody (Novus, NB100-142), anti-MDC antibody (Bethyl, b13423), anti-53BP1 antibody (SantaCruz, sc-22760), anti-Rap80 antibody (Bethyl, A300-763A), anti-ATM p1981 antibody (Abcam, ab36810), FITC-conjugated anti-BrdU antibody (BD biosciences), mouse anti-RPA antibody (Sigma). Anti-mouse IgG-Cy3 antibody (Sigma, c2181), anti-rabbit IgG-FITC antibody (Sigma, f7512), anti-rabbit IgG-Cy3 antibody (Sigma, and C2306), anti-mouse IgG-FITC antibody (Sigma, F6257).

Complementation assays

To test whether sRNAs can complement the reduction in HR repair caused by the depletion of Dicer. In total, 1×10^6 U2OS/DR-GFP cells were seeded in six-well plates. Twenty-four hours after transfection with Dicer siRNAs, U2OS/DR-GFP cells were co-transfected with 2 μg pCBA-I-SceI and Dicer siRNAs, after another 48 h, permeabilized with 1% Tween 20 in PBS for 15 min at room temperature and incubated 15 min at room temperature with 50 ng (except for the dose response experiment in Supplementary information, Figure S1G where 50 ng, 20 ng or 5 ng sRNAs were used) purified sRNAs in DMEM (final concentration on cells was 0.25 ng/μl). sRNAs were extracted from U2OS/DR-GFP cells transfected with pCBA-I-SceI or empty vector. Cells were then left to recover for 1 h in DMEM with 10% fetal bovine serum at 37 °C, 5% CO₂, and processed for flow cytometric analysis of GFP. We verified that the permeabilization treatment did not induce severe cell stress by comparing cell death in treated and untreated samples (Supplementary information, Figure S3C).

Acknowledgments

We are grateful to Drs M Jasin, L Du, X Li for providing the reagents or technical support. This work was supported by the National Basic Research Program of China (973 Program, 2011CB510103 to Y-GY, 2012CB910900 to YQ), the National Natural Science Foundation of China (31225015 to YQ, 31370796 to Y-GY, 31150110143 to JMRD), the CAS Young Foreign Fellow

Award (2010Y2SB14 to JMRD), the Danish Council for Independent Research - Medical Sciences (JMRD), the CAS "100-talents" Professor Program (Y-GY).

References

- Wyman C, Kanaar R. DNA double-strand break repair: all's well that ends well. *Annu Rev Genet* 2006; **40**:363-383.
- Hoeijmakers JH. Genome maintenance mechanisms for preventing cancer. *Nature* 2001; **411**:366-374.
- Jackson SP, Bartek J. The DNA-damage response in human biology and disease. *Nature* 2009; **461**:1071-1078.
- Wei W, Ba Z, Gao M, et al. A role for small RNAs in DNA double-strand break repair. *Cell* 2012; **149**:101-112.
- Lieber MR1, Ma Y, Pannicke U, Schwarz K. Mechanism and regulation of human non-homologous DNA end-joining. *Nat Rev Mol Cell Biol* 2003; **4**:712-720.
- San Filippo J, Sung P, Klein H. Mechanism of eukaryotic homologous recombination. *Annu Rev Biochem* 2008; **77**:229-257.
- Ciccio A, Elledge SJ. The DNA damage response: making it safe to play with knives. *Mol Cell* 2010; **40**:179-204.
- D'Amours D, Jackson SP. The Mre11 complex: at the crossroads of dna repair and checkpoint signalling. *Nat Rev Mol Cell Biol* 2002; **3**:317-327.
- Gravel S1, Chapman JR, Magill C, Jackson SP. DNA helicases Sgs1 and BLM promote DNA double-strand break resection. *Genes Dev* 2008; **22**:2767-2772.
- Mimitou EP, Symington LS. Sae2, Exo1 and Sgs1 collaborate in DNA double-strand break processing. *Nature* 2008; **455**:770-774.
- Sartori AA, Lukas C, Coates J, et al. Human CtIP promotes DNA end resection. *Nature* 2007; **450**:509-514.
- Carthew RW, Sontheimer EJ. Origins and mechanisms of miRNAs and siRNAs. *Cell* 2009; **136**:642-655.
- Francia S, Michelini F, Saxena A, et al. Site-specific DICER and DROSHA RNA products control the DNA-damage response. *Nature* 2012; **488**:231-235.
- Michalik KM, Bottcher R, Forstemann K. A small RNA response at DNA ends in *Drosophila*. *Nucleic Acids Res* 2012; **40**:9596-9603.
- Pierce AJ, Johnson RD, Thompson LH, Jasin M. XRCC3 promotes homology-directed repair of DNA damage in mammalian cells. *Genes Dev* 1999; **13**:2633-2638.
- Bennardo N, Cheng A, Huang N, Stark JM. Alternative-NHEJ is a mechanistically distinct pathway of mammalian chromosome break repair. *PLoS Genet* 2008; **4**:e1000110.
- Plath KES, Grabbe J, Gibbs BF. Calcineurin antagonists differentially affect mediator secretion, p38 mitogen-activated protein kinase and extracellular signal-regulated kinases from immunologically activated human basophils. *Clin Exp Allergy* 2003; **33**:342-350.
- Silva J, Mak W, Zvetkova I, Appanah R, et al. Establishment of histone H3 methylation on the inactive X chromosome requires transient recruitment of Eed-Enx1 Polycomb group complexes. *Dev Cell* 2003; **4**:481-495.
- Rinn JL, Kertesz M, Wang JK, et al. Functional demarcation of active and silent chromatin domains in human HOX loci by noncoding RNAs. *Cell* 2007; **129**:1311-1323.
- Hale CR, Zhao P, Olson S, et al. RNA-guided RNA cleavage by a CRISPR RNA-Cas protein complex. *Cell* 2009; **139**:945-956.
- Lukas J, Lukas C, Bartek J. More than just a focus: the chromatin response to DNA damage and its role in genome integrity maintenance. *Nat Cell Biol* 2011; **13**:1161-1169.
- Chapman JR, Taylor MR, Boulton SJ. Playing the end game: DNA double-strand break repair pathway choice. *Mol Cell* 2012; **47**:497-510.
- Liu J, Carmell MA, Rivas FV, et al. Argonaute2 is the catalytic engine of mammalian RNAi. *Science* 2004; **305**:1437-1441.
- Ma JB, Ye K, Patel DJ. Structural basis for overhang-specific small interfering RNA recognition by the PAZ domain. *Nature* 2004; **429**:318-322.
- Kawamata T, Tomari Y. Making RISC. *Trends Biochem Sci* 2010; **35**:368-376.
- Meister G, Landthaler M, Patkaniowska A, Dorsett Y, Teng G, Tuschl T. Human Argonaute2 mediates RNA cleavage targeted by miRNAs and siRNAs. *Mol Cell* 2004; **15**:185-197.
- Fabian MR, Sonenberg N, Filipowicz W. Regulation of mRNA translation and stability by microRNAs. *Annu Rev Biochem* 2010; **79**:351-379.
- Xia B, Sheng Q, Nakanishi K, et al. Control of BRCA2 cellular and clinical functions by a nuclear partner, PALB2. *Mol Cell* 2006; **22**:719-729.
- Hutvagner G, McLachlan J, Pasquinelli AE, Bálint E, Tuschl T, Zamore PD. A cellular function for the RNA-interference enzyme Dicer in the maturation of the let-7 small temporal RNA. *Science* 2001; **293**:834-838.
- Fang L, Wang Y, Du D, et al. Cell polarity protein Par3 complexes with DNA-PK via Ku70 and regulates DNA double-strand break repair. *Cell Res* 2007; **17**:100-116.
- Yu X, Chen J. DNA damage-induced cell cycle checkpoint control requires CtIP, a phosphorylation-dependent binding partner of BRCA1 C-terminal domains. *Mol Cell Biol* 2004; **24**:9478-9486.

(Supplemental information is linked to the online version of the paper on the *Cell Research* website.)



This work is licensed under the Creative Commons Attribution-NonCommercial-No Derivative Works 3.0 Unported License. To view a copy of this license, visit <http://creativecommons.org/licenses/by-nc-nd/3.0>